

APC: Adaptive Patch Contrast for Weakly Supervised Semantic Segmentation

Wangyu Wu^{1,2}, Tianhong Dai³, Zhenhong Chen⁴,
Xiaowei Huang², Fei Ma^{1*}, Jimin Xiao^{1*}

¹Xi'an Jiaotong-Liverpool University, Suzhou, China.

²University of Liverpool, Liverpool, UK.

³University of Aberdeen, Aberdeen, UK.

⁴Microsoft, Redmond, USA.

*Corresponding author(s). E-mail(s): fei.ma@xjtlu.edu.cn;
jimin.xiao@xjtlu.edu.cn;

Contributing authors: wangyu.wu22@student.xjtlu.edu.cn;
tianhong.dai@abdn.ac.uk; zcheh@microsoft.com;
xiaowei.huang@liverpool.ac.uk;

Abstract

Weakly Supervised Semantic Segmentation (WSSS) using only image-level labels has gained significant attention due to its cost-effectiveness. The typical framework involves using image-level labels as training data to generate pixel-level pseudo-labels with refinements. Recently, methods based on Vision Transformers (ViT) have demonstrated superior capabilities in generating reliable pseudo-labels, particularly in recognizing complete object regions, compared to CNN methods. However, current ViT-based approaches have some limitations in the use of patch embeddings, being prone to being dominated by certain abnormal patches, as well as many multi-stage methods being time-consuming and lengthy in training, thus lacking efficiency. Therefore, in this paper, we introduce a novel ViT-based WSSS method named *Adaptive Patch Contrast* (APC) that significantly enhances patch embedding learning for improved segmentation effectiveness. APC utilizes an Adaptive-K Pooling (AKP) layer to address the limitations of previous max pooling selection methods. Additionally, we propose a Patch Contrastive Learning (PCL) to enhance patch embeddings, thereby further improving the final results. Furthermore, we improve upon the existing multi-stage training framework without CAM by transforming it into an end-to-end single-stage training approach, thereby enhancing training efficiency. The experimental results show that our approach is effective and efficient, outperforming

other state-of-the-art WSSS methods on the PASCAL VOC 2012 and MS COCO 2014 dataset within a shorter training duration.

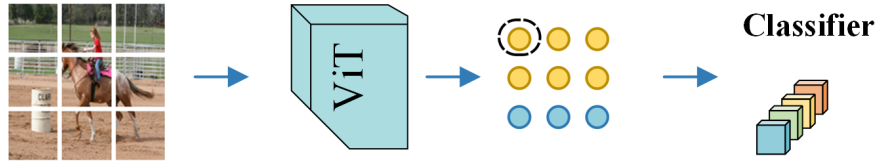
Keywords: Weakly-Supervised Learning, Semantic Segmentation, contrastive learning, vision transformer

1 Introduction

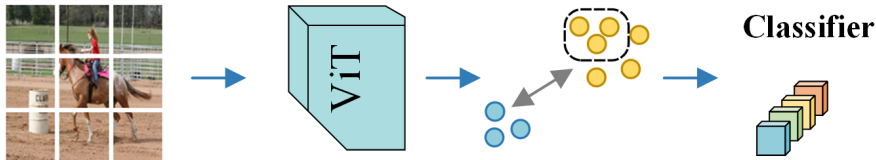
Semantic segmentation [1, 2] is an important task in the field of computer vision. Weakly Supervised Semantic Segmentation (WSSS) is a continuously evolving approach in this field, which aims to generate pixel-level labels by utilizing weak supervision signals to significantly reduce the cost of annotations. Classic weak supervision signals include image-level labels [3], points [4], scribbles [5], and bounding boxes [6]. Among the various weak supervision signals, most recent research has focused on the image-level label, primarily because it is the cheapest and contains the least information. This work also falls within the domain of WSSS, where it exclusively utilizes image-level labels.

Prevalent works of WSSS approaches relying on image-level class labels typically generate pseudo labels using class activation maps (CAM) [7]. However, CAMs have limitations in accurately estimating both the shape and localization of objects belonging to the classes of interest [8]. This has prompted researchers to incorporate additional refinements between the initial pseudo labels and the final pseudo labels generation. These refinements often involve multi-stage architectures, as observed in PAMR [9], thereby increasing complexity. Notable refinement strategies have been described in IRNet [10] and AdvCAM [11]. However, these multi-stage architectures greatly impact computational performance, leading to inefficient training. In recent years, due to the limitations of CAM, researchers have turned to leverage ViT-based frameworks for WSSS [12–15]. ViT-PCM [12] utilizes patch embeddings to infer the probability of pixel-level labels. Methods such as [13, 14] use ViT to replace CNN, thereby enhancing CAM’s capability in object recognition. Additionally, AFA [15] proposes an end-to-end architecture based on CAM and suggests acquiring reliable semantic affinity through attention blocks to enhance the initial coarse labels. However, current ViT-based methods utilize global max pooling to select the patch with the highest prediction score, projecting patch-level classification to image-level, which may impact final performance due to misclassification. Moreover, frameworks without CAM are still in multi-stage training, requiring the separate generation of initial pseudo labels before proceeding to the next stage of training, which lacks efficiency.

In this work, we empirically observe that existing ViT frameworks without CAM utilize a max pooling layer to connect image embedding patches with softmax, representing the probabilities of different image categories. However, max pooling has limitations as it may be dominated by individual outlier patches, lacking robustness. Additionally, the current ViT framework without CAM involves multi-stage training, requiring training to be conducted separately in different stages, significantly impacting training efficiency. Therefore, we propose an effective approach called *Adaptive*



(a) ViT - max pooling



(b) APC - Adaptive Patch Contrast



Fig. 1: In the case of predicting the specific category 'horse': (a) The previous ViT-based method [16] only projects the class prediction of a single patch with the highest prediction score into the image-level classification. (b) Our APC projects the class prediction from adaptive K patches into the image-level classification and utilizes patch contrastive learning to enhance patch embeddings.

K pooling with patch contrastive learning, as illustrated in Figure 1, to address the aforementioned issue. Firstly, we propose an Adaptive-K Pooling (AKP) module to overcome the limitations of max pooling by replacing it with a adaptive-k pooling layer. This helps in mitigating the potential influence of individual outlier points and better represents the impact of different objects on the final prediction in images containing multiple objects. Specifically, in the AKP module, the original max pooling is replaced with a top-K pooling layer, where an adaptive algorithm based on numerical differences selects the optimal K value, addressing the issue of single-point dependence. Furthermore, to effectively combat the issue of over-smoothing, we propose a Patch Contrastive Learning (PCL) module to enhance intra-class compactness and inter-class separability, thereby generating more accurate patch predictions. In the PCL module, we calculate pairwise cosine similarities for patch embeddings generated by ViT, bringing closer the distances in the embedding space for the same category and increasing the distances between different classes, effectively improving the final performance. Additionally, to further enhance the effectiveness of the previous without

CAM framework, based on the proposed AKP and PCL, we construct an end-to-end single-stage WSSS framework without CAM and achieve significant improvements in computational performance.

Overall, the contributions of our work can be summarized as follows:

1) We propose a novel ViT-based framework that does not utilize CAM. By incorporating adaptive-k pooling, we address the issue of inaccurate final label predictions, which are influenced by individual misclassified patches

2) We propose a patch-based contrastive learning module, in which we introduce the Patch Contrastive Learning (PCL). By computing the cosine similarity between patch pairs, we aim to increase the distance between patch pairs of different classes and reduce the distance between patch pairs of the same class, thereby enhancing the intra-class compactness and inter-class separability of patch embeddings and further improving the quality of pseudo labels.

3) We propose an end-to-end single-stage training framework based on ViT without CAM. This framework addresses the issue of multi-stage inefficiency in previous frameworks without CAM. In our experiments, our proposed approach outperforms other state-of-the-art methods for segmentation tasks on the PASCAL VOC 2012 [17] and MS COCO 2014 dataset [18].

2 Related work

2.1 WSSS with Image-level Labels

Existing WSSS methods commonly rely on image-level class labels as the cheapest form of supervision. Approaches using image-level class labels have traditionally been based on CAM methods [7], employing a standard multi-label classification network. The CAMs are derived by applying global average pooling (GAP) to the feature maps of the last layer, followed by concatenation into a weights vector. This vector is then connected to the class prediction through Binary Cross-Entropy (BCE) prediction loss. A common limitation of CAM is its tendency to activate only the most discriminative object regions. To address this limitation, recent studies have proposed various training strategies, including techniques such as erasing [19], online attention accumulation [20], and cross-image semantic mining [21]. Researchers in [22] suggest leveraging auxiliary tasks to regularize the training objective, such as learning visual words. Contrast pixel and prototype representations [23, 24] to promote the comprehensive activation of object regions. Typically, these methods are built upon the CAM framework, constrained by the drawbacks of CAM.

To enable the network to capture more object parts, researchers have introduced greater challenges to the classification objective. This has been achieved by modifying either the input data [19, 25–28] or the feature maps [29–31], employing techniques like dropping out parts of the image or introducing perturbations. Some studies [22] have made the classification task more difficult by adding finer-grained categories. Additionally, information across multiple images has been used to improve CAM maps [21, 32].

The CAM framework remains limited by its tendency to activate only the most discriminative object regions. Hence, we propose a novel WSSS framework not based

on CAM. We utilize Vision Transformer (ViT) to generate image patch embeddings and then utilize Adaptive K pooling to predict the categories of each patch. Finally, we map the patches to pixels as the segmentation result to address the limitation of CAM activating only the most discriminative object regions.

2.2 Vision Transformers

Vision Transformer (ViT)[16] has achieved notable success across a range of vision tasks[16, 33]. This success has led to the adoption of ViT in Weakly Supervised Semantic Segmentation (WSSS), where ViT-based methods have begun to emerge as alternatives to traditional CNN-based approaches for generating Class Activation Maps (CAMs)[14, 15]. Among these approaches are models like MCTformer[14] and AFA [15], which, despite leveraging ViT, still rely on CAMs. MCTformer utilizes ViT’s attention mechanism to generate localization maps and employs PSA [3] for generating pseudo-masks. Similarly, AFA takes advantage of ViT’s multi-head self-attention to gain global insights and uses an affinity module to propagate pseudo-masks.

Another approach, ViT-PCM [12], departs from this reliance on CAMs by using patch embeddings and max pooling to infer the probability of pixel-level labels. This marks a significant development as it is the first instance of employing a framework that does not depend on CAMs to generate baseline pseudo-masks in WSSS. However, this reliance on max pooling can lead to issues, particularly when patches are misclassified.

In contrast to these methods, our approach employs ViT as the backbone and incorporates adaptive K pooling for the first time. This innovation addresses the limitations associated with max pooling and the potential for misclassification of patches within a framework that does not rely on CAM. Additionally, we introduce the Patch-level Contrastive Learning (PCL) module, which enhances intra-class compactness and inter-class separability of patch embeddings. This further improves the quality of the final labels, providing a more robust and accurate framework for WSSS without relying on CAMs.

2.3 Single-stage WSSS methods

Single-stage WSSS methods unify multiple stages such as classification, pseudo-label refinement, and segmentation into a single joint training process, greatly enhancing training efficiency compared to the previous multi-stage frameworks. 1Stage [9] achieves performance comparable to mainstream multi-stage methods by ensuring local consistency, semantic fidelity, and mask completeness. AFA [15] explores the intrinsic architecture of ViT and extracts reliable semantic affinity from multi-head self-attention for pseudo-label refinement. ToCo [13] addresses the observed issue of excessive smoothing in ViT by supervising the final patch tokens with intermediate knowledge. Despite the simplified and streamlined training process of single-stage methods, they typically do not perform as well as multi-stage methods. In this work, we not only enhance the accuracy of patch prediction to pixel in the without CAM framework but also achieve superior semantic segmentation results using a single-stage framework.

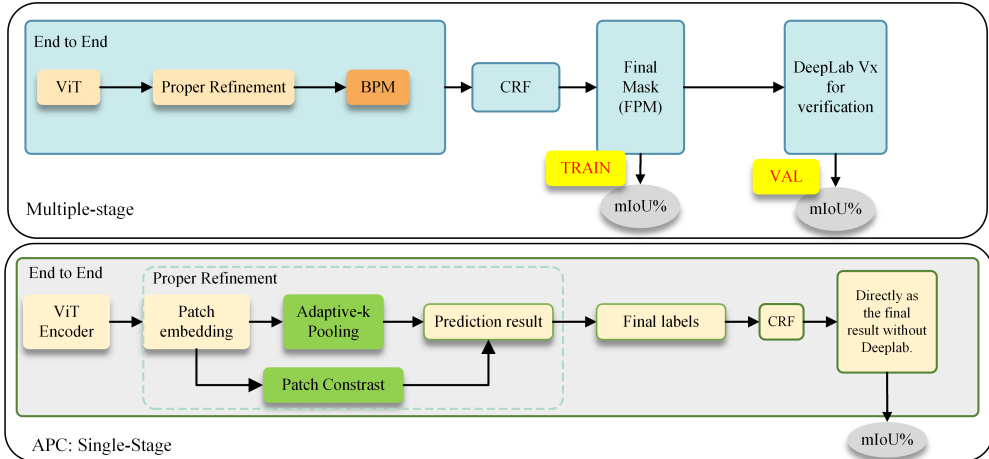


Fig. 2: The figure compares the basic structure of a multiple-stage WSSS method, depicted in light blue at the top, with our proposed APC method, shown in light gray at the bottom. APC, based on the ViT framework without CAM, eliminates the need for multi-stage learning during training. By adopting a single-stage approach, we can directly obtain final labels without further processing, and they can be directly used for verification without the need for an additional selected semantic segmentation model (i.e., DeepLab [34]) task. In contrast to APC, current methods without CAM require multi-stage optimization. All recent methods require refining the BPM with a CRF [35] before passing them to the verification task.

3 Method

In this section, we introduce the overall structure and key components of our proposed method. Initially, in Section 3.1, we provide an overview of the APC method and compare it with the existing multi-stage approaches. Subsequently, in Section 3.2, we detail the specifics of our model framework, including how to obtain image patch embeddings from images and how to perform segmentation tasks. We have enhanced the existing non-CAM multi-stage framework into a single-stage framework, incorporating a segmentation decoder that utilizes a decoder head to merge multi-level feature maps for prediction, implemented through simple MLP layers. In Section 3.3, we describe the proposed adaptive K pooling layer, which selects the final prediction patches by choosing different K values based on the ratio of prediction scores, aiming to address incorrect predictions dominated by a single patch. Furthermore, in Section 3.4, we discuss the integration of contrastive learning into our current framework. We introduce patch-level contrastive learning, calculating the cosine similarity for pairs of patch embeddings produced by ViT. We define patch contrastive learning (PCL) to enhance patch representations, reduce the distance between patches of the same category, and increase the distance between patches of different categories, thereby further improving prediction accuracy. Finally, in Section 3.5, we will summarize our APC overall loss.

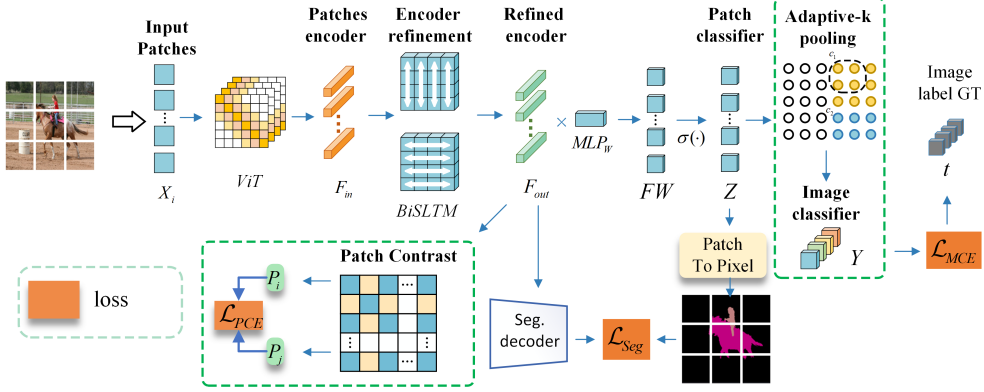


Fig. 3: The detailed infrastructure of APC is as follows. Initially, APC employs ViT as an encoder to generate patch embeddings. This is followed by the use of BiLSTM to further refine the patch encoder. Subsequently, patch-to-classifier predictions are obtained through MLP and softmax activation. In the adaptive-K pooling module, a mapping from the patch classifier to the image classifier is established, leveraging the image-level GT label for model supervision. Furthermore, after the Refined Encoder stage, a patch contrastive learning (PCL) is introduced to enhance the integration of similarity among patches. Finally, the refined patch embeddings are used as input for the segmentation decoder to compute the segmentation loss. The supervision for the segmentation branch is provided by the label refined through the Patch to Pixel module.

3.1 Overall Framework

Our proposed APC method mainly consists of three main components: the adaptive K pooling module, the image patch contrastive module, and the end-to-end encoder and decoder module, as illustrated in Figure 2. We first compare with the previous without CAM multiple-stage framework, where our significant improvement lies in transforming the entire WSSS process into a single stage. By introducing the encoder and decoder modules, we enable the framework to directly predict segmentation results during training. Next, we delve into the main proper refinement component of APC. In the first stage, the input image is divided into fixed-size patches, and then a ViT encoder is used to generate an embedding for each patch. Each patch here is represented as an embedding space vector. To further enhance the performance of the patch classifier, adaptive K pooling is employed for patch selection specific to certain categories, and these selected patches are then used for prediction. Additionally, we introduce the patch contrastive module, which adjusts the cosine similarity of patch embeddings belonging to the same categories to be closer and that of patch embeddings belonging to different categories to be farther apart. Through the aforementioned modules, our method obtains prediction results, which are directly used as final labels.

After refinement with CRF, they are directly used as the final output for verification without the need for an additional DeepLab task.

3.2 Model Structure

This section provides a comprehensive explanation regarding the generation of patch embeddings and the design of the end-to-end single-stage WSSS task. The illustration of details about this method is shown in Figure 3. The input image $X_{in} \in \mathbb{R}^{h \times w \times 3}$ is firstly divided into s fixed-size input patches $X_{patch} \in \mathbb{R}^{d \times d \times 3}$, where $s = \frac{hw}{d^2}$. Then, the input patches X_{patch} are passed into ViT-based encoder to generate the patch embeddings $F_{in} \in \mathbb{R}^{s \times e}$. Next, HV-BiLSTM is used to enhance the representation of F_{in} and output refined patch embeddings F_{out} with the same size as F_{in} . Given the refined patch embedding F_{out} , we use a weight $W \in \mathbb{R}^{e \times |\mathcal{C}|}$ and a softmax activation function to predict the class $c \in \mathcal{C}$ of each patch, where $|\mathcal{C}|$ is the total number of classes:

$$Z = \text{softmax}(F_{out}W). \quad (1)$$

The output $Z \in \mathbb{R}^{s \times |\mathcal{C}|}$ represents the prediction scores of each class for each patch. To robustly project from patch-level predictions to image-level predictions, we propose an adaptive K pooling module, described in Sec.3.3. The adaptive K module selects the top k patches $\{\bar{Z}_{i=1:k}^c\}$ with the highest value in each category and computes the average value as the prediction score for image-level classification:

$$y_c = \frac{1}{k} \sum_{i=1}^k \bar{Z}_i^c, \quad (2)$$

where y_c is the projected image-level prediction score of class c . Adaptive K pooling ensures the final image prediction results are not dominated by any misclassified patches, thereby further improving the mapping from patch-level prediction to image-level prediction. We compute the distance between each patch pair using cosine similarity on the patch embeddings after refinement, and then apply contrastive learning, detailed in Section 3.4. Simultaneously, we introduce a decoder head to merge multi-level feature patch embeddings for prediction, implemented through a simple MLP layer. The decoder’s prediction is combined with our patch prediction category result to calculate the segmentation loss L_{seg} , where the predicted category of each patch is directly mapped onto each pixel within the patch as the pixel’s category for calculating the segmentation loss. For the segmentation loss L_{seg} , we utilize the commonly used cross-entropy loss. As illustrated in Figure 3, the supervision for the segmentation branch is the label refined through the Patch to Pixel module.

Finally, we minimize the error between the predicted image labels y_c and ground-truth labels t_c by using the multi-label classification prediction error (MCE):

$$\begin{aligned} \mathcal{L}_{MCE} &= \frac{1}{|\mathcal{C}|} \sum_{c \in \mathcal{C}} BCE(t_c, y_c) \\ &= -\frac{1}{|\mathcal{C}|} \sum_{c \in \mathcal{C}} t_c \log(y_c) + (1 - t_c) \log(1 - y_c). \end{aligned} \quad (3)$$

We use binary labels and C independent Bernoulli distributions to model multi-label classification. With C representing the number of classes, C binary cross-entropy losses (BCE) measure the dissimilarity between predicted and ground-truth labels.

3.3 Patch Embeddings with Adaptive K Pooling

The motivation behind using Adaptive K pooling is to facilitate the mapping between patch-level classification and image-level classification. In previous work [12], Global Max Pooling (GMP) only selects the patches with the highest prediction scores for each class, which may result in inaccurate mapping of patch-level predictions to image-level classification. In our experiments, we observed that some patches are misclassified with high prediction scores, and when there are multiple objects of the same categories in an image, a single patch as a prediction score may not effectively represent the overall mapping of the image to these categories. Therefore, to achieve a more robust mapping between patch-level and image-level classification, we average the prediction scores of the top k patches in each category as the prediction score for image-level classification. Additionally, we propose an adaptive algorithm to automatically select the value of k based on different scenarios, instead of using a fixed value of k . This allows for more flexible adaptation to various scenarios.

The illustration of details about this method is shown in Figure 3. The output $Z \in \mathbb{R}^{s \times |C|}$ represents the prediction scores for each class for each patch. We replace the original max pooling layer with an adaptive K pooling layer to map the patch category predictions of the entire image to image category predictions. Regarding the selection of K, we propose an adaptive K pooling module, described in Algorithm 1.

In our observation, we found that for each patch generating predictions for a specific category Z , in images containing multiple objects, besides the patch with the maximum prediction score, patches with prediction scores close to the maximum score also represent the category well. We designed an adaptive algorithm that automatically expands the selected set when it detects patches with prediction scores close to the maximum score and the difference between them is less than θ .

3.4 Patch Contrastive Learning

To enhance the representation of patch embeddings and thus improve the accuracy of prediction, the patch contrastive learning (PCL) is used to narrow the distance between patch embeddings with high prediction scores in a specific category c and also expand the distance between patch embeddings with high scores and the low confidence patch embeddings in the same category. In this work, cosine similarity is used to measure the distance between patch embeddings:

$$S(F_{out}^i, F_{out}^j) = \frac{F_{out}^i \cdot F_{out}^j}{\|F_{out}^i\| \|F_{out}^j\|}, \quad (4)$$

where a higher similarity value means two patch embeddings are closer to each other, and a lower value indicates a further distance. To represent the similarity more explicitly, we normalize the range of value between 0 and 1 via:

Algorithm 1: Adaptive K selection

Input: *input_tensor* of patch-to-categories prediction scores, number of categories C

Output: *AdaptiveK_candidate* after adaptive K selection

```
1 AdaptiveK_candidate  $\leftarrow \emptyset$ 

2 foreach category  $c_i$  in  $C$  do
3   selected_elements  $\leftarrow$  top-1 values of input_tensor for category  $c_i$ 

4   for  $i \leftarrow 2$  to  $K$  do
5     current_elements  $\leftarrow$  top- $i$  values of input_tensor for category  $c_i$ 
6     mean_current  $\leftarrow$  compute mean of current_elements
7     mean_selected  $\leftarrow$  compute mean of selected_elements
8     if  $\frac{\text{mean\_selected}}{\text{mean\_current}} > \theta$  then
9       selected_elements  $\leftarrow$  current_elements

10  AdaptiveK_candidate[ $c_i$ ]  $\leftarrow$  selected_elements

11 return AdaptiveK_candidate
```

$$\bar{S}(F_{out}^i, F_{out}^j) = \frac{1 + S(F_{out}^i, F_{out}^j)}{2}. \quad (5)$$

As illustrated in Figure 3, F_{out} is used as the input of PCL module. Furthermore, the patch prediction score Z_i^c and a threshold ϵ are used to determine whether a patch is a high confidence one $\mathcal{P}_{high}^c = \{F_{out}^i | Z_i^c > \epsilon\}$. Similarly, the patch with the lowest prediction score is considered as a low confidence one $\mathcal{P}_{low}^c = \{F_{out}^i | Z_i^c < (1 - \epsilon)\}$. Then, the patch contrastive learning error (PCE) of a category c can be expressed as:

$$\begin{aligned} \mathcal{L}_{PCE}^c &= \frac{1}{N_{pair}^+} \sum_{i=1}^{|\mathcal{P}_{high}^c|} \sum_{j=1, j \neq i}^{|\mathcal{P}_{high}^c|} (1 - \bar{S}(F_{high}^i, F_{high}^j)) \\ &+ \frac{1}{N_{pair}^-} \sum_{m=1}^{|\mathcal{P}_{high}^c|} \sum_{n=1}^{|\mathcal{P}_{low}^c|} \bar{S}(F_{high}^m, F_{low}^n), \end{aligned} \quad (6)$$

where N_{pair}^+ denotes the number of pairs of patches with high confidence, N_{pair}^- denotes the number of pairs of high confidence and low confidence patches. F_{high} and F_{low} represent the feature embeddings of high confidence patch \mathcal{P}_{high}^c and low confidence patch \mathcal{P}_{low}^c , respectively.

3.5 Overall loss

As illustrated in Figure 3, we have introduced multiple losses in the previous sections, including the contrastive learning L_{pce} loss, the classification L_{mce} loss, and the segmentation loss L_{seg} . The overall loss of our APC is the weighted sum of L_{pce} , L_{mce} , and L_{seg} :

$$\mathcal{L} = \mathcal{L}_{mce} + \lambda_1 \mathcal{L}_{seg} + \lambda_2 \sum_{c \in \mathcal{C}} \mathcal{L}_{PCE}^c, \quad (7)$$

where λ_1 , and λ_2 balance the contributions of different losses.

4 Experiments

In this section, we describe the experimental settings, including dataset, evaluation metrics, and implementation details. We then compare our method with state-of-the-art approaches on PASCAL VOC 2012 dataset [17] and MS COCO 2014 [18]. Finally, ablation studies are performed to validate the effectiveness of crucial components in our proposed method.

Table 1: Impact of hyper-parameters. The performance is evaluated on the VOC val set. The default settings are marked in baseline color gray.

Size	Seg.
640 ²	71.6
800 ²	72.1
960 ²	72.3
1120 ²	72.0

(a) The size of the image in the inference stage.

λ_1	Seg.
0.1	71.6
0.15	72.0
0.2	72.3
0.25	71.8

(b) The different values of λ_1 .

λ_2	Seg.
0.05	71.3
0.08	71.8
0.1	72.3
0.12	72.0

(c) The different values of λ_2 .

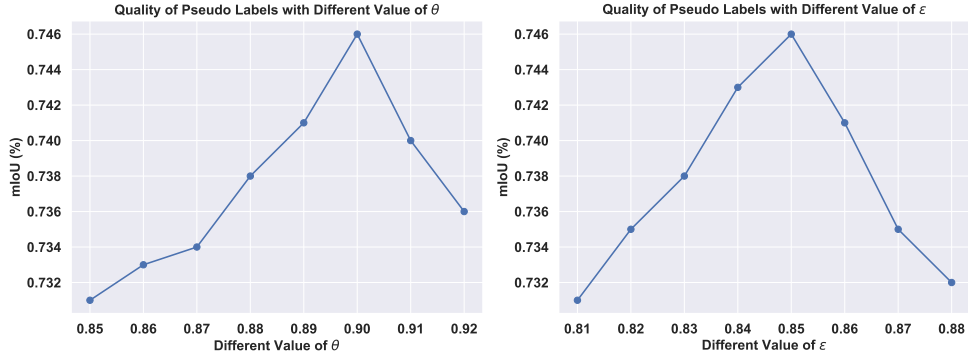


Fig. 4: The performance comparison of selecting different values of θ and ϵ .

Table 2: Results of predicted pseudo masks on PASCAL VOC 2012 train.

Method	Pub.	Backbone	mIoU (%)
SEAM [36]	CVPR20	V1-RN38	63.6
CONTA [37]	NeurIPS20	V1-RN38	67.9
CDA [38]	ICCV21	V1-RN38	66.4
EPS [39]	CVPR21	V2-RN101	71.4
Yao <i>et al.</i> [40]	CVPR21	V2-RN101	68.3
AuxSegNet [41]	ICCV21	V1-RN38	69.0
AdvCAM [42]	PAMI22	V2-RN101	69.9
PPC [24]	CVPR22	ResNet38	61.5
SIPE [23]	CVPR22	ResNet50	58.6
AFA [15]	CVPR22	MiT-B1	66.0
ViT-PCM [16]	ECCV22	ViT-B/16	71.4
ToCo [13]	CVPR23	ViT-B/16	72.2
USAGE [43]	ICCV23	ResNet38	72.8
FPR [44]	ICCV23	ResNet38	68.5
APC (Ours)		ViT-B/16	74.6

4.1 Experimental Settings

Dataset and Evaluated Metric. Our experiments are conducted on two benchmark datasets: PASCAL VOC 2012 [17], which includes 21 classes, and MS COCO 2014 [18], featuring 81 classes. Each dataset also contains an extra class for background. The PASCAL VOC 2012 dataset is commonly expanded using the SBD dataset [45]. For training on PASCAL VOC 2012, we use 10,582 images with image-level labels and 1,449 images for the validation set. In the case of the MS COCO 2014 dataset, approximately 82k images are used for training and around 40k images for validation, with the training images having only image-level annotations. The performance is evaluated using the mean Intersection-Over-Union (mIoU) metric. Our APC approach demonstrates substantial improvements in segmentation results on both PASCAL VOC 2012 and MS COCO 2014 datasets.

Implementation Details. In our experiments, we utilize the ViT-B/16 model as the backbone for the ViT encoder. During the training process, input images are initially resized to 384×384 , as suggested in Kolesnikov et al. (2016) [46], and subsequently partitioned into 24×24 small patches for the ViT encoder. For the inference stage, we resize the image to 960×960 . The model is trained with a batch size of 16 and for a maximum of 50 epochs, utilizing two NVIDIA 4090 GPUs. We employ the Adam optimizer and schedule the learning rate as follows: the learning rate is set to 10^{-3} for the first two epochs, and then to 10^{-4} for the remaining epochs. We set the threshold ϵ to 0.85 to determine high-confidence patches in PCE, and k is set to 6 for adaptive-K pooling. The impact of hyper-parameters is assessed on the VOC val set, with default settings indicated in baseline color gray, as illustrated in Table 1. The default weight coefficients λ_1 and λ_2 are set to 0.02 and 0.01, respectively, and θ is set to 0.9. As shown in Figure 4, the performance is compared by selecting different values for θ and ϵ . During the validation phase, we do not require additional DeepLab training for full supervision. Instead, we directly use the model’s prediction results as the final labels and validate them on the validation set.

Table 3: Final Semantic segmentation performance for training on Pascal VOC 2012 val.

Model	Pub.	Backbone	mIoU (%)
<i>Multiple-Stage method</i>			
CIAN [32]	AAAI20	V2-RN101	64.3
ICD [47]	CVPR20	V2-RN101	67.8
Zhang <i>et al.</i> [48]	ECCV20	ResNet50	66.6
Sun <i>et al.</i> [21]	ECCV20	V2-RN101	66.2
SEAM [36]	CVPR20	V1-RN38	64.5
CONTA [37]	NeurIPS20	V1-RN38	66.1
EDAM [49]	CVPR21	V2-RN101	70.9
EPS [39]	CVPR21	V2-RN101	71.0
Yao <i>et al.</i> [40]	CVPR21	V2-RN101	68.3
AuxSegNet [41]	ICCV21	V1-RN38	69.0
CDA [38]	ICCV21	V1-RN38	66.1
AdvCAM [42]	PAMI22	V2-RN101	68.1
Li <i>et al.</i> [50]	CVPR22	V2-RN101	72.0
Du <i>et al.</i> [24]	CVPR22	V2-RN101	72.6
RCA [51]	CVPR22	V2-RN38	72.2
L2G [52]	CVPR22	V1-RN38	72.0
MCTformer [14]	CVPR22	DeiT-S	61.7
SIPE [23]	CVPR22	ResNet50	58.6
ViT-PCM [16]	ECCV22	ViT-B/16	69.3
USAGE [43]	ICCV23	ResNet38	71.9
SAS [53]	AAAI23	ViT-B/16	69.5
FPR [44]	ICCV23	ResNet38	70.0
<i>End-To-End Single-Stage</i>			
AFA [15]	CVPR22	MiT-B1	63.8
ToCo [13]	CVPR23	ViT-B/16	70.5
TSCD [54]	AAAI23	MiT-B1	67.3
APC (Ours)		ViT-B/16	72.3

4.2 Comparisons with State-of-the-art

Comparison of Pseudo Masks. We evaluated the performance of our APC method on the PASCAL VOC 2012 dataset for pseudo mask prediction, using 10,582 images with only image-level labels to train the segmentation network. Subsequently, we conducted segmentation predictions on these 10,582 images. As demonstrated in Table 2, our APC method outperforms other state-of-the-art techniques, encompassing both multi-stage and single-stage approaches, by achieving an mIoU value of 74.6% on the training data. This achievement is credited to our proposed adaptive-K pooling method, which dynamically selects an optimal number of K patches for category prediction scores, effectively addressing the challenge of mapping patch-level classification to image-level classification using a single patch’s prediction score. Additionally, the incorporation of patch contrastive learning further boosts the overall performance.

Table 4: Final Semantic segmentation performance for training on MS COCO 2014 val set.

Model	Pub.	Backbone	mIoU (%)
<i>Multiple-Stage method</i>			
Luo <i>et al.</i> [55]	AAAI20	V2-VGG16	29.9
SEAM [36]	CVPR20	V1-RN38	31.9
CONTA [37]	NeurIPS20	V1-RN38	32.8
EPS [39]	CVPR21	V2-VGG16	35.7
RCA [51]	CVPR22	V2-VGG16	36.8
AuxSegNet [41]	ICCV21	V1-RN38	33.9
Wang <i>et al.</i> [56]	IJCV20	V2-VGG16	27.7
Kweon <i>et al.</i> [57]	ICCV21	V1-RN38	36.4
CDA [38]	ICCV21	V1-RN38	33.2
AdvCAM [11]	CVPR21	V2-RN101	44.4
Li <i>et al.</i> [50]	CVPR22	V2-RN101	44.7
L2G [52]	CVPR22	V2-RN101	44.2
MCTformer [14]	CVPR22	Resnet38	42.0
ViT-PCM [16]	ECCV22	ViT-B/16	45.0
SIPE [23]	CVPR22	Resnet38	43.6
OCR [58]	CVPR23	ViT-B/16	42.5
SAS [53]	AAAI23	ViT-B/16	44.8
FPR [44]	ICCV23	ResNet38	43.9
<i>End-To-End Single-Stage</i>			
AFA [15]	CVPR22	MiT-B1	38.9
ToCo [13]	CVPR23	ViT-B/16	42.3
TSCD [54]	AAAI23	MiT-B1	40.1
APC (Ours)		ViT-B/16	45.7

Comparison of Segmentation Results. In this study, we compared the final segmentation performance of our proposed APC end-to-end method on the PASCAL VOC 2012 and MS COCO 2014 datasets. As shown in Table 3, consistent with other comparative methods, we utilized 10,582 images with only image-level labels as the training set to train our APC model. For validation, we employed 1,449 images to

assess our final semantic segmentation performance, where our end-to-end single-stage method outperformed both recent end-to-end approaches and multiple-stage methods. Notably, the end-to-end method significantly surpasses multiple-stage methods in computational efficiency, offering substantial savings in capacity. These details will be further elaborated in Section 4.3. Regarding the MS COCO 2014 dataset, we adopted a similar approach, using approximately 82k images for training and around 40k images for validation to evaluate the final semantic segmentation performance. As indicated in Table 4, our method continued to exhibit superior performance.

4.3 Ablation Studies

Table 5: Ablation studies on computational efficiency for Pascal VOC 2012: Time elapsed from the start of training to the achievement of final semantic segmentation results.

Multiple-Stage	End-to-End	AKP	PCL	Cost Time (Hours)
✓				8±1
	✓			4±1
	✓	✓		3±0.5
	✓	✓	✓	1.5±0.5

Table 6: Ablation studies on different pooling strategies for final semantic segmentation performance on Pascal VOC 2012 val.

PCL	Average pooling	Max-Pooling	Top-K	AKP	mIoU(%)
✓	✓				61.7%
✓		✓			70.5%
✓			✓		71.8%
✓				✓	72.3%

Performance and Computational Efficiency. Table 5 demonstrates the superiority of our APC in terms of computational performance. We conducted ablation experiments comparing multiple-stage methods with our end-to-end single-stage module, Adaptive-K Pooling (AKP) module, and Patch Contrastive Learning (PCL) module. For the sake of fairness in experimentation, all comparisons were conducted on a single NVIDIA 4090 GPU machine. As shown in Table 5, traditional multiple-stage methods typically require over 8 hours, as they involve training pseudo-labels in the first stage and then utilizing them as training data for fully supervised deeplab network training, consuming significant computational resources. With the introduction of the end-to-end method, the time significantly reduced to around 4 hours. Subsequently, incorporating the AKP module further reduced the time to approximately 3 hours. Finally, with the addition of contrastive learning, significant performance

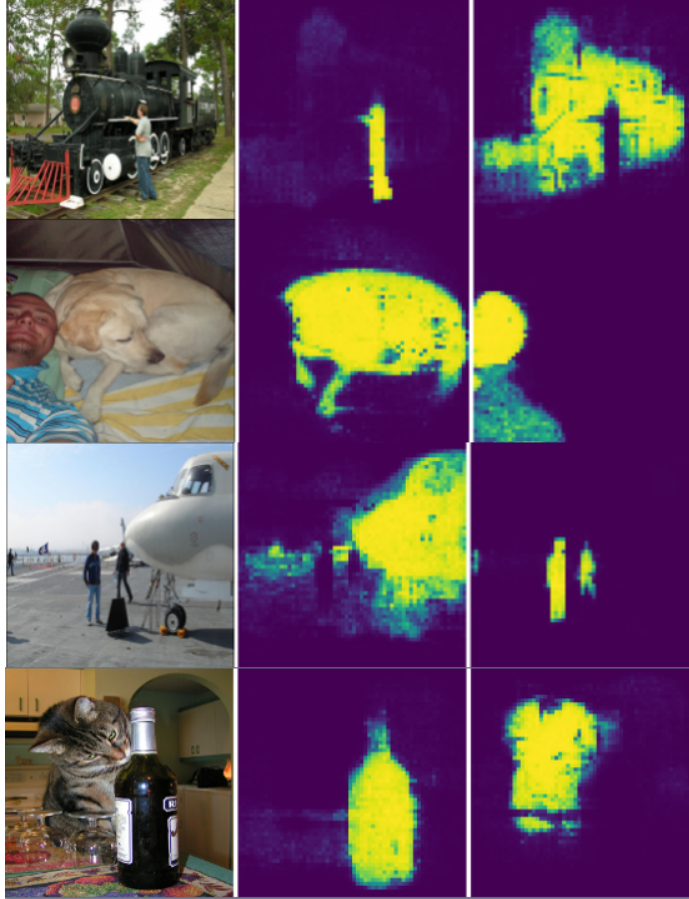


Fig. 5: The sample illustrates probabilities highlighted by 60×60 heatmaps, which are generated from the patch to pixel module to produce pixel probabilities.

improvements were achieved, with faster convergence typically observed within about 15 epochs. The total time required was approximately 1.5 hours. Experimental results indicate that our approach not only greatly enhances the final segmentation performance but also significantly improves computational speed, thereby saving more computational resources.

The Impact of Different Pooling Strategies. Table 6 presents ablation studies on various pooling strategies for final semantic segmentation performance. We compared the performance of average pooling layer, max pooling layer, fixed top-K pooling layer, and our proposed adaptive-K pooling layer. To ensure fair experimentation, we incorporated the PCL module and utilized an end-to-end framework in all cases. The only difference lies in the choice of pooling layer. The experiments were conducted on the Pascal VOC 2012 validation dataset. We observed that our proposed adaptive-K pooling achieved the highest performance.



Fig. 6: The comparison of qualitative segmentation results from top to bottom: the images, GT, max-pooling (ViT-PCM [16]), ViT+AKP, and our APC utilizing ViT+AKP+PCL.

Table 7: Ablation studies on AKP and PCL for final semantic segmentation performance on Pascal VOC 2012 val.

Backbone	Max-Pooling	AKP	PCL	Seg mIoU (%)
ViT-B/16	✓			68.6%
ViT-B/16		✓		70.3%
ViT-B/16		✓	✓	72.3%

The Impact of Different component. Ablation studies were conducted to verify the effectiveness of two key components of our proposed method: AKP and PCL. As shown in Table 7, Adaptive-K pooling improves the final segmentation performance by 1.7% mIoU compared to max pooling. Additionally, by incorporating the proposed PCL, the segmentation task performance further improved by 2.0% mIoU. Therefore, these two components significantly contribute to outperforming previous ViT-based methods in our approach.

4.4 Visualization Results

Visualization of Heatmaps. We present the results of heatmap visualization in Figure 5, where probabilities are highlighted by 60×60 heatmaps. Pixels with values in yellow indicate the probability of belonging to the predicted class.

Segmentation Visualization Results. We present the final semantic segmentation results in Figure 6. Concurrently, we compared these results with those from the previous max pooling-based method, demonstrating a significant improvement in semantic segmentation performance.

5 Conclusion

In this work, we propose APC approach without using CAM for weakly supervised semantic segmentation. Unlike previous methods, APC utilizes adaptive-K pooling to select k patches for mapping patch-level classification to image-level classification, thus mitigating the issue of potential misclassified patches. In addition, patch contrastive learning (PCL) is proposed to further enhance the feature embeddings of patches. In the same class, PCL aims to decrease the distance between patch embeddings with high confidence and increase the distance between embeddings with high confidence and embeddings with low confidence. By combining these two components, our method achieves state-of-the-art results in weakly supervised semantic segmentation tasks using only image-level labels.

6 Declarations

- **Funding:** The work was supported by National Key R&D Program of China (No.2022YFE0200300), National Natural Science Foundation of China under 61972323, and XJTLU AI University Research Centre, Jiangsu Province Engineering Research Centre of Data Science and Cognitive Computation at XJTLU and SIP AI innovation platform (YZCXPT2022103).
- **Competing interests:** All authors certify that they have no affiliations with or involvement in any organization or entity with any financial interest or non-financial interest in the subject matter or materials discussed in this manuscript.
- **Ethics approval:** Not applicable.
- **Consent to participate:** Not applicable.
- **Consent for publication:** Not applicable.
- **Authors' contribution:** Wangyu Wu: Data curation, Formal analysis, Methodology, Experiment, Validation, Writing – original draft. Tianhong Dai, Zhenhong Chen, Xiaowei Huang, Fei Ma and Jimin Xiao: Conceptualization, Methodology, Resources, Supervision, Writing – review & editing.
- **Data availability and access:** We use two datasets: PASCAL VOC 2012 [17] with SBD [45] and MS COCO-2014 [18]. All of them are from public resources. The PASCAL VOC 2012 dataset generated and analyzed during the current study is available in the PASCAL repository [17], which is from the following public domain resources: <http://host.robots.ox.ac.uk/pascal/VOC/voc2012/index.html>. The dataset SBD (Hariharan et al., 2011) is available at the following public domain resources: <http://home.bharathh.info/pubs/codes/SBD/download.html>. The MS COCO-2014 dataset generated and analyzed during the current study is available in COCO repository (Lin et al., 2014), which is from the following public domain resources: <https://cocodataset.org/>.

References

- [1] Yue, W., Zhou, Z., Cao, Y., Wu, W.: Visual representations with texts domain generalization for semantic segmentation. *Applied Intelligence* (2023)
- [2] Wang, H., Cao, G., Cao, W.: A novel inference paradigm based on multi-view prototypes for one-shot semantic segmentation. *Applied Intelligence* (2023)
- [3] Ahn, J., Kwak, S.: Learning pixel-level semantic affinity with image-level supervision for weakly supervised semantic segmentation. In: *Proc. IEEE Conf. Comput. Vis. Pattern Recog.*, pp. 4981–4990 (2018)
- [4] Bearman, A., Russakovsky, O., Ferrari, V., Fei-Fei, L.: What’s the point: Semantic segmentation with point supervision. In: *Eur. Conf. Comput. Vis.*, pp. 549–565 (2016). Springer
- [5] Zhang, B., Xiao, J., Zhao, Y.: Dynamic feature regularized loss for weakly supervised semantic segmentation. *arXiv preprint arXiv:2108.01296* (2021)
- [6] Lee, J., Yi, J., Shin, C., Yoon, S.: Bbam: Bounding box attribution map for weakly supervised semantic and instance segmentation. In: *Proc. IEEE Conf. Comput. Vis. Pattern Recog.*, pp. 2643–2652 (2021)
- [7] Zhou, B., Khosla, A., Lapedriza, A., Oliva, A., Torralba, A.: Learning deep features for discriminative localization. In: *Proc. IEEE Conf. Comput. Vis. Pattern Recog.*, pp. 2921–2929 (2016)
- [8] Chen, Z., Wang, T., Wu, X., Hua, X.-S., Zhang, H., Sun, Q.: Class re-activation maps for weakly-supervised semantic segmentation. In: *Proc. IEEE Conf. Comput. Vis. Pattern Recog.*, pp. 969–978 (2022)
- [9] Araslanov, N., Roth, S.: Single-stage semantic segmentation from image labels. In: *Proc. IEEE Conf. Comput. Vis. Pattern Recog.*, pp. 4253–4262 (2020)
- [10] Ahn, J., Cho, S., Kwak, S.: Weakly supervised learning of instance segmentation with inter-pixel relations. In: *Proc. IEEE Conf. Comput. Vis. Pattern Recog.*, pp. 2209–2218 (2019)
- [11] Lee, J., Kim, E., Yoon, S.: Anti-adversarially manipulated attributions for weakly and semi-supervised semantic segmentation. In: *Proc. IEEE Conf. Comput. Vis. Pattern Recog.*, pp. 4071–4080 (2021)
- [12] Rossetti, S., Zappia, D., Sanzari, M., Schaerf, M., Pirri, F.: Max pooling with vision transformers reconciles class and shape in weakly supervised semantic segmentation. In: *Eur. Conf. Comput. Vis.*, pp. 446–463 (2022)
- [13] Ru, L., Zheng, H., Zhan, Y., Du, B.: Token contrast for weakly-supervised semantic segmentation. In: *Proc. IEEE Conf. Comput. Vis. Pattern Recog.*, pp.

- [14] Xu, L., Ouyang, W., Bennamoun, M., Boussaid, F., Xu, D.: Multi-class token transformer for weakly supervised semantic segmentation. In: Proc. IEEE Conf. Comput. Vis. Pattern Recog., pp. 4310–4319 (2022)
- [15] Ru, L., Zhan, Y., Yu, B., Du, B.: Learning affinity from attention: End-to-end weakly-supervised semantic segmentation with transformers. In: Proc. IEEE Conf. Comput. Vis. Pattern Recog., pp. 16846–16855 (2022)
- [16] Dosovitskiy, A., Beyer, L., Kolesnikov, A., Weissenborn, D., Zhai, X., Unterthiner, T., Dehghani, M., Minderer, M., Heigold, G., Gelly, S., et al.: An image is worth 16x16 words: Transformers for image recognition at scale. arXiv preprint arXiv:2010.11929 (2020)
- [17] Everingham, M., Van Gool, L., Williams, C.K., Winn, J., Zisserman, A.: The pascal visual object classes (VOC) challenge. *Int. J. Comput. Vis.* **88**, 303–338 (2010)
- [18] Lin, T.-Y., Maire, M., Belongie, S., Hays, J., Perona, P., Ramanan, D., Dollár, P., Zitnick, C.L.: Microsoft coco: Common objects in context. In: Eur. Conf. Comput. Vis., pp. 740–755 (2014). Springer
- [19] Wei, Y., Feng, J., Liang, X., Cheng, M.-M., Zhao, Y., Yan, S.: Object region mining with adversarial erasing: A simple classification to semantic segmentation approach. In: Proc. IEEE Conf. Comput. Vis. Pattern Recog., pp. 1568–1576 (2017)
- [20] Jiang, P.-T., Hou, Q., Cao, Y., Cheng, M.-M., Wei, Y., Xiong, H.-K.: Integral object mining via online attention accumulation. In: Proceedings of the IEEE/CVF International Conference on Computer Vision, pp. 2070–2079 (2019)
- [21] Sun, G., Wang, W., Dai, J., Van Gool, L.: Mining cross-image semantics for weakly supervised semantic segmentation. In: Computer Vision—ECCV 2020: 16th European Conference, Glasgow, UK, August 23–28, 2020, Proceedings, Part II 16, pp. 347–365 (2020). Springer
- [22] Chang, Y.-T., Wang, Q., Hung, W.-C., Piramuthu, R., Tsai, Y.-H., Yang, M.-H.: Weakly-supervised semantic segmentation via sub-category exploration. In: Proc. IEEE Conf. Comput. Vis. Pattern Recog., pp. 8991–9000 (2020)
- [23] Chen, Q., Yang, L., Lai, J.-H., Xie, X.: Self-supervised image-specific prototype exploration for weakly supervised semantic segmentation. In: Proc. IEEE Conf. Comput. Vis. Pattern Recog., pp. 4288–4298 (2022)
- [24] Du, Y., Fu, Z., Liu, Q., Wang, Y.: Weakly supervised semantic segmentation by pixel-to-prototype contrast. In: Proc. IEEE Conf. Comput. Vis. Pattern Recog.,

- pp. 4320–4329 (2022)
- [25] Singh, K.K., Lee, Y.J.: Hide-and-seek: Forcing a network to be meticulous for weakly-supervised object and action localization. In: Proc. IEEE Int. Conf. Comput. Vis. (2017)
 - [26] Wu, W., Dai, T., Huang, X., Ma, F., Xiao, J.: Image augmentation with controlled diffusion for weakly-supervised semantic segmentation. In: IEEE Int. Conf. Acoust. Speech Signal Process. (2024)
 - [27] Zhang, F., Gu, C., Zhang, C., Dai, Y.: Complementary patch for weakly supervised semantic segmentation. In: Proc. IEEE Int. Conf. Comput. Vis., pp. 7242–7251 (2021)
 - [28] Li, K., Wu, Z., Peng, K.-C., Ernst, J., Fu, Y.: Tell me where to look: Guided attention inference network. In: Proc. IEEE Conf. Comput. Vis. Pattern Recog., pp. 9215–9223 (2018)
 - [29] Lee, J., Kim, E., Lee, S., Lee, J., Yoon, S.: Ficklenet: Weakly and semi-supervised segmentation using stochastic inference. In: Proc. IEEE Conf. Comput. Vis. Pattern Recog., pp. 5267–5276 (2019)
 - [30] Hou, Q., Jiang, P., Wei, Y., Cheng, M.-M.: Self-erasing network for integral object attention. In: Int. Conf. Neur. Info. Process. Sys., pp. 547–557 (2018)
 - [31] Choe, J., Shim, H.: Attention-based dropout layer for weakly supervised object localization. In: Proc. IEEE Conf. Comput. Vis. Pattern Recog. (2019)
 - [32] Fan, J., Zhang, Z., Tan, T., Song, C., Xiao, J.: Cian: Cross-image affinity net for weakly supervised semantic segmentation. In: AAAI Conf. Artif. Intell., vol. 34, pp. 10762–10769 (2020)
 - [33] Carion, N., Massa, F., Synnaeve, G., Usunier, N., Kirillov, A., Zagoruyko, S.: End-to-end object detection with transformers. In: Eur. Conf. Comput. Vis., pp. 213–229 (2020). Springer
 - [34] Chen, L.-C., Papandreou, G., Kokkinos, I., Murphy, K., Yuille, A.L.: Deeplab: Semantic image segmentation with deep convolutional nets, atrous convolution, and fully connected crfs. *IEEE Trans. Pattern Anal. Mach. Intell.* **40**(4), 834–848 (2017)
 - [35] Krähenbühl, P., Koltun, V.: Efficient inference in fully connected crfs with gaussian edge potentials. In: Int. Conf. Neur. Info. Process. Sys., vol. 24 (2011)
 - [36] Wang, Y., Zhang, J., Kan, M., Shan, S., Chen, X.: Self-supervised equivariant attention mechanism for weakly supervised semantic segmentation. In: Proc. IEEE Conf. Comput. Vis. Pattern Recog., pp. 12275–12284 (2020)

- [37] Zhang, D., Zhang, H., Tang, J., Hua, X., Sun, Q.: Causal intervention for weakly-supervised semantic segmentation. In: *Int. Conf. Neur. Info. Process. Sys.*, vol. 33, pp. 655–666 (2020)
- [38] Su, Y., Sun, R., Lin, G., Wu, Q.: Context decoupling augmentation for weakly supervised semantic segmentation. In: *Proc. IEEE Int. Conf. Comput. Vis.*, pp. 7004–7014 (2021)
- [39] Lee, S., Lee, M., Lee, J., Shim, H.: Railroad is not a train: Saliency as pseudo-pixel supervision for weakly supervised semantic segmentation. In: *Proc. IEEE Conf. Comput. Vis. Pattern Recog.*, pp. 5495–5505 (2021)
- [40] Yao, Y., Chen, T., Xie, G.-S., Zhang, C., Shen, F., Wu, Q., Tang, Z., Zhang, J.: Non-salient region object mining for weakly supervised semantic segmentation. In: *Proc. IEEE Conf. Comput. Vis. Pattern Recog.*, pp. 2623–2632 (2021)
- [41] Xu, L., Ouyang, W., Bennamoun, M., Boussaid, F., Sohel, F., Xu, D.: Leveraging auxiliary tasks with affinity learning for weakly supervised semantic segmentation. In: *Proc. IEEE Int. Conf. Comput. Vis.*, pp. 6984–6993 (2021)
- [42] Lee, J., Kim, E., Mok, J., Yoon, S.: Anti-adversarially manipulated attributions for weakly supervised semantic segmentation and object localization. *IEEE Trans. Pattern Anal. Mach. Intell.* (2022)
- [43] Peng, Z., Wang, G., Xie, L., Jiang, D., Shen, W., Tian, Q.: Usage: A unified seed area generation paradigm for weakly supervised semantic segmentation. In: *Proc. IEEE Int. Conf. Comput. Vis.*, pp. 624–634 (2023)
- [44] Chen, L., Lei, C., Li, R., Li, S., Zhang, Z., Zhang, L.: Fpr: False positive rectification for weakly supervised semantic segmentation. In: *Proc. IEEE Int. Conf. Comput. Vis.*, pp. 1108–1118 (2023)
- [45] Hariharan, B., Arbeláez, P., Bourdev, L., Maji, S., Malik, J.: Semantic contours from inverse detectors. In: *Proc. IEEE Int. Conf. Comput. Vis.*, pp. 991–998 (2011)
- [46] Kolesnikov, A., Lampert, C.H.: Seed, expand and constrain: Three principles for weakly-supervised image segmentation. In: *Eur. Conf. Comput. Vis.*, pp. 695–711 (2016)
- [47] Fan, J., Zhang, Z., Song, C., Tan, T.: Learning integral objects with intra-class discriminator for weakly-supervised semantic segmentation. In: *Proc. IEEE Conf. Comput. Vis. Pattern Recog.*, pp. 4283–4292 (2020)
- [48] Zhang, T., Lin, G., Liu, W., Cai, J., Kot, A.: Splitting vs. merging: Mining object regions with discrepancy and intersection loss for weakly supervised semantic segmentation. In: *Eur. Conf. Comput. Vis.*, pp. 663–679 (2020)

- [49] Wu, T., Huang, J., Gao, G., Wei, X., Wei, X., Luo, X., Liu, C.H.: Embedded discriminative attention mechanism for weakly supervised semantic segmentation. In: Proc. IEEE Conf. Comput. Vis. Pattern Recog., pp. 16765–16774 (2021)
- [50] Li, J., Fan, J., Zhang, Z.: Towards noiseless object contours for weakly supervised semantic segmentation. In: Proceedings of the IEEE/CVF Conference on Computer Vision and Pattern Recognition, pp. 16856–16865 (2022)
- [51] Zhou, T., Zhang, M., Zhao, F., Li, J.: Regional semantic contrast and aggregation for weakly supervised semantic segmentation. In: Proceedings of the IEEE/CVF Conference on Computer Vision and Pattern Recognition, pp. 4299–4309 (2022)
- [52] Jiang, P.-T., Yang, Y., Hou, Q., Wei, Y.: L2g: A simple local-to-global knowledge transfer framework for weakly supervised semantic segmentation. In: Proceedings of the IEEE/CVF Conference on Computer Vision and Pattern Recognition, pp. 16886–16896 (2022)
- [53] Kim, S., Park, D., Shim, B.: Semantic-aware superpixel for weakly supervised semantic segmentation. In: AAAI Conf. Artif. Intell., vol. 37, pp. 1142–1150 (2023)
- [54] Xu, R., Wang, C., Sun, J., Xu, S., Meng, W., Zhang, X.: Self correspondence distillation for end-to-end weakly-supervised semantic segmentation. In: AAAI Conf. Artif. Intell., vol. 37, pp. 3045–3053 (2023)
- [55] Luo, W., Yang, M.: Learning saliency-free model with generic features for weakly-supervised semantic segmentation. In: AAAI Conf. Artif. Intell., vol. 34, pp. 11717–11724 (2020)
- [56] Wang, G., Wang, G., Zhang, X., Lai, J., Yu, Z., Lin, L.: Weakly supervised person re-id: Differentiable graphical learning and a new benchmark. *IEEE Trans. Neural Netw. Learn. Syst.* **32**(5), 2142–2156 (2020)
- [57] Kweon, H., Yoon, S.-H., Kim, H., Park, D., Yoon, K.-J.: Unlocking the potential of ordinary classifier: Class-specific adversarial erasing framework for weakly supervised semantic segmentation. In: Proc. IEEE Int. Conf. Comput. Vis., pp. 6994–7003 (2021)
- [58] Cheng, Z., Qiao, P., Li, K., Li, S., Wei, P., Ji, X., Yuan, L., Liu, C., Chen, J.: Out-of-candidate rectification for weakly supervised semantic segmentation. In: Proc. IEEE Conf. Comput. Vis. Pattern Recog., pp. 23673–23684 (2023)